Uwe Schroeder, Monica Materano, Terence Mittmann, Patrick D. Lomenzo, Thomas Mikolajick, Akira Toriumi

Recent progress for obtaining the ferroelectric phase in hafnium oxide based films: impact of oxygen and zirconium

Erstveröffentlichung in / First published in:

Japanese Journal of Applied Physics. 2019, 58, S. SL0801-1 - SL0801-7 {Zugriff am: 09.11.2022}. IOP Publishing. ISSN 1347-4065.

DOI: http://dx.doi.org/10.7567/1347-4065/ab45e3

Final edited form was published in "Japanese Journal of Applied Physics". 2019, 58, S. SL0801-1 - SL0801-7. ISSN 1347-4065.
http://dx.doi.org/10.7567/1347-4065/ab45e3

Recent progress for obtaining the ferroelectric phase in hafnium oxide based films: impact of oxygen and zirconium

Uwe Schroeder[1*], Monica Materano[1], Terence Mittmann[1], Patrick D. Lomenzo[1], Thomas Mikolajick[1,2], and Akira Toriumi[1,2,3]

[1]*Namlab gGmbH, Noethnitzer Strasse 64, 01187 Dresden, Germany*
[2]*TU Dresden, IHM, Chair of Nanoelectronic Materials, Noethnitzer Strasse 64, 01187 Dresden, Germany*
[3]*The University of Tokyo, Bunkyo, Tokyo 113-8656, Japan*

[*]E-mail: uwe.schroeder@namlab.com

Different causes for ferroelectric properties in hafnium oxide were discussed during the last decade including various dopants, stress, electrode materials, and surface energy from different grain sizes. Recently, the focus shifted to the impact of oxygen vacancies on the phase formation process. In this progress report, the recent understanding of the influence of oxygen supplied during deposition on the structural phase formation process is reviewed and supplemented with new data for mixed HfxZr1-xOy films. Even though polar and non-polar HfxZr1-xOy thin films are well characterized, little is known about the impact of oxygen exposure during the deposition process. Here, a combination of structural and electrical characterization is applied to investigate the influence of the oxygen and zirconium content on the crystallization process during ALD deposition in comparison to other deposition techniques. Different polarization properties are assessed which correlate to the determined phase of the film. Optimized oxygen pulse times can enable the crystallization of HfxZr1-xOy in a polar orthorhombic phase rather than a non-polar monoclinic and tetragonal phase.

1. Introduction

During recent years, the interest in the phase formation process for thin doped HfO_2 and $Hf_xZr_{1-x}O_2$ (HZO with $0 \leqslant x \leqslant 1$) mixed films has increased drastically because of the impact on the recently discovered ferroelectric (FE) properties[1)] for these oxide systems. The FE properties in such simple oxide systems enhance the possibilities to integrate FE films into CMOS processes.[2)] Various dopants[1,3–6)] showed an enhancement of the FE properties in thin HfO_2 films within a certain process window for different deposition techniques like atomic layer deposition (ALD),[7)] sputter deposition (PVD),[8)] molecular beam epitaxy,[9)] chemical solution deposition,[10)] and pulsed laser deposition (PLD).[11)] Within the literature, various factors in addition to dopants were discussed for the cause of the ferroelectric properties in these layers including stress,[12)] electrode materials,[13)] annealing/quenching[14)] and surface/interface energy of the grains in the polycrystalline structure of the HfO_2 films.[15)] Recently, the impact of oxygen vacancies on the phase formation process is analyzed in detail[16,17)] and will be reviewed in the following text.

Within this report the HZO system is chosen as a reference system for ferroelectric doped HfO_2 films. Before the initial paper by Boescke et al.[1)] only non-polar dielectric properties were related to the monoclinic (m−) phase for hafnium-rich mixed HZO films and the tetragonal (t−) phase for high ZrO_2 content[18,19)] with a transition to the cubic (c−) phase e.g. for Y doped ZrO_2.[20)] Since then, the dependence of the dielectric and FE properties on the Hf/Zr content is typically presented with paraelectric characteristics for the m-phase in HfO_2 rich films, the highest remanent and saturation polarization for HZO with about 50% ZrO_2 content related to the orthorhombic (o−) $Pbc2_1$ phase[3)]. Almost no remanent polarization but still high saturation polarization (mixed o/t-phase) is formed for pure ZrO_2[3,21)] and yet no ferroelectric properties for e.g. yttrium stabilized ZrO_2 (o/t-phase).[14)] The amount of remanent polarization for pure ZrO_2 depends on the substrate or different interfacial layers. Lu and Hsu et al. reported stable FE properties with remanent polarization values of 20 μC cm^{-2} for ZrO_2 deposited on a Pt(111) surface and similar P_r values for ZrO_2 fabricated on a HfO_2 interlayer on a TiN bottom electrode.[22,23)] Substrate and interfacial layers that do not scavenge oxygen from films (e.g. Pt) seem to stabilize a ferroelectric phase in ZrO_2 in contrast to substrates that pull oxygen out of the layer (e.g. TiN) which cause the formation of an o/t-phase with pinched hysteresis loops.[24)]

These results indicate the strong impact of oxygen on the phase formation process. Several authors reported changes in the phase formation for pure HfO_2 without looking at the FE properties.[25–29)] Here, clear indications for a t- to m- phase change for higher O content are discussed for thin HfO_2 films in resistive switching applications.[27,28)] Similar phase differences are seen for FE devices showing an improvement of the FE properties for O deficient HfO_2 films deposited by ALD[16)] and PVD.[17)] Investigations into thin PECVD ZrO_2 on Si, again confirmed a film crystallinity change from the t- to the m-phase[30)] for higher O content.

In the following sections, a detailed review of ALD in relation to the sputter process conditions on the phase formation in the mixed oxide system is presented to obtain an understanding of the impact of Hf, Zr, and O content on crystal phase formation.

2. Experimental methods

TiN/HZO/TiN capacitor stacks are fabricated on Si substrates by first depositing a 10 nm thick sputter deposited TiN layer using a Ti target in N_2 plasma at room temperature. Afterwards, 10 nm HZO films are deposited by ALD using TEMAHf ($Hf[N(CH_3)(C_2H_5)]_4$) and $CpZr[N(CH_3)_2]_3$ as metal precursors and O_3 as an oxygen source at a deposition temperature of 230 °C (HfO_2), 280 °C (HZO), and 300 °C (ZrO_2) in a showerhead based ALD tool manufactured by Meyer Burger. For HfO_2 lower deposition temperatures are used to avoid early crystallization. Similar results can be also reached by using other Hf, Zr or O precursors by different

Final edited form was published in "Japanese Journal of Applied Physics". 2019, 58, S. SL0801-1 - SL0801-7. ISSN 1347-4065.
http://dx.doi.org/10.7567/1347-4065/ab45e3

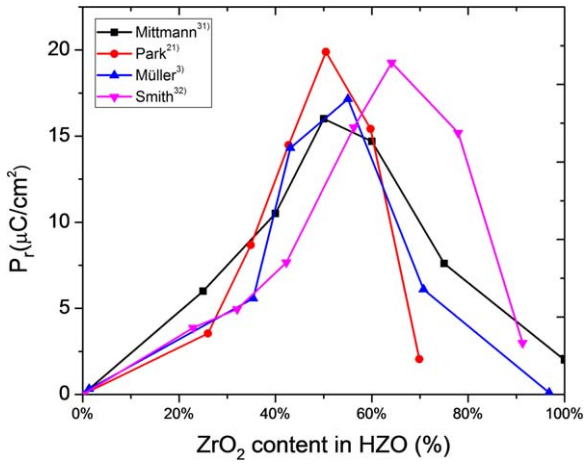

Fig. 1. (Color online) Remanent polarization (P_r) as a function of different $Hf_xZr_{1-x}O_2$ composition as published by different authors.[3,21,31,32)]

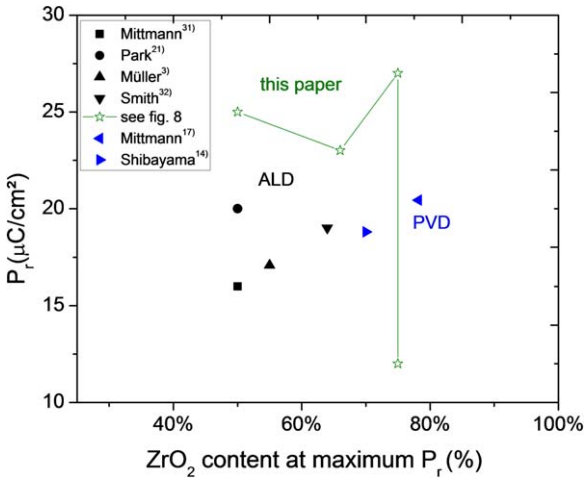

Fig. 2. (Color online) Maximum P_r versus ZrO_2 content in HZO of Fig. 1[3,21,31,32)] together with results for PVD films[14,17)] in comparison to ALD results with different O_3 pulse times as shown in Fig. 8.

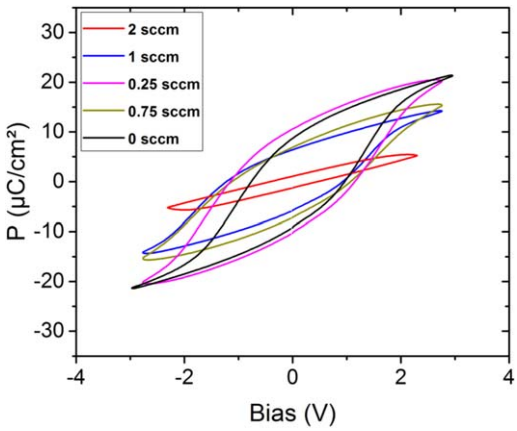

Fig. 3. (Color online) Polarization versus applied voltage hysteresis for $TiN/HfO_2/TiN$ capacitors with different O_2 flow during PVD HfO_2[17)] deposition.

authors (e.g. TEMAZr,[21,31)] TDMAHf,[32,33)] TDMAZr[32,33)] as shown in Fig. 1. Higher HfO_2 contents in the layer required lower deposition temperatures to reduce initial crystallization. Different Hf/Zr ratios are reached by changing the Hf to Zr pulse ratio. The oxygen content within the HZO layer is varied by adjusting the O_3 pulse time. The growth rates of the pure HfO_2 and ZrO_2 ALD processes were determined as 0.08 nm/cycle and 0.07 nm/cycle, respectively. The absolute number of ALD cycles defines the thickness of the film with a target thickness of about 10 nm. All films were almost amorphous after deposition, requiring a crystallization anneal to achieve ferroelectric behavior (see also discussion of Fig. 5). The top TiN electrode is again deposited by sputter deposition at room temperature followed by a rapid thermal crystallization anneal at 600 °C for 20 s in N_2. In the following step, 10 nm Ti/25 nm Pt dots are deposited through a shadow mask to define the pad with a size of 200 μm in diameter. These pads are separated by an SC1 clean. For structural film analysis, a Bruker D8 Discover X-ray diffraction (XRD) tool (Cu–K_α radiation: 0.154 nm wavelength) was used to determine the crystallographic structure in addition to film thickness and density by X-ray reflectometry. Ferroelectric properties including remanent polarization P_r, and coercive field E_c, were measured on the capacitors with an AixACCT TFA3000 ferroelectric tester. *P–E* hysteresis loops were performed at 1 kHz using a triangular voltage signal at 3 MV cm^{-1}. Only for pure ZrO_2 a field of 4 MV cm^{-1} is supplied to better show the pinched hysteresis loop properties.

3. Results and discussion

As discussed in the introduction, various authors published the impact of the Hf/Zr composition on the remanent polarization of the material in a TiN electrode based capacitor stack and gained different results as shown in Fig. 1. In all cases a minimum in the polarization is visible for high HfO_2 and ZrO_2 content.[3,21,31,32)] Maximum values are reached for different ZrO_2 contents in HfO_2 (Fig. 2).

Adding similar data for PVD deposited HZO layers,[14,17)] the maximum P_r value can be found in a wide range of Hf/Zr composition from 50% to ~80% ZrO_2 content. So far no reason for this differences is discussed in literature. All ALD films are deposited 260 °C–300 °C in contrast to PVD layer, which are fabricated at room temperature to gain best amorphous properties of the films. In both cases a broad intensity background is visible in XRD indicating very small crystallites. Experiments for pure HfO_2 revealed a strong impact for different O_2 flows during PVD HfO_2[17,29)] (Fig. 3) and O_3 pulse times in ALD HfO_2 deposition.[16)]

For pure ZrO_2, structural differences are discussed by Cho et al. in PECVD deposited ZrO_2 films on Si[25)] and PLD deposited ZrO_2 nanostructures,[34)] showing a change in the phase from t- to m-phase for higher O content. In addition, main differences in FE properties are accomplished for different bottom electrodes (TiN versus Pt),[33)] interface layers (TiO_2, HfO_2),[33)] or different deposition temperature (150 °C versus 300 °C).[22,23)] Electrodes (e.g. Pt) and interfaces (e.g. HfO_2), that enhance the O content in ZrO_2 result in a reduction of the t-phase and enhanced o-phase content with higher FE properties. All factors seem to impact the nucleation and film growth behavior resulting in different ZrO_2 phases and FE properties (Fig. 4).

Due to the ambiguity in process details of previous work by different authors, new results are presented here to distinguish between the impact of Zr and oxygen content within a HfO_2 layer in between TiN electrodes after 600 °C anneal on the crystal phase formation process. GIXRD diffraction patterns are measured to analyze the HZO phase content for different O or Zr compositions. The oxygen content within HZO is varied by changing the O_3 pulse time.

Final edited form was published in "Japanese Journal of Applied Physics". 2019, 58, S. SL0801-1 - SL0801-7. ISSN 1347-4065.
http://dx.doi.org/10.7567/1347-4065/ab45e3

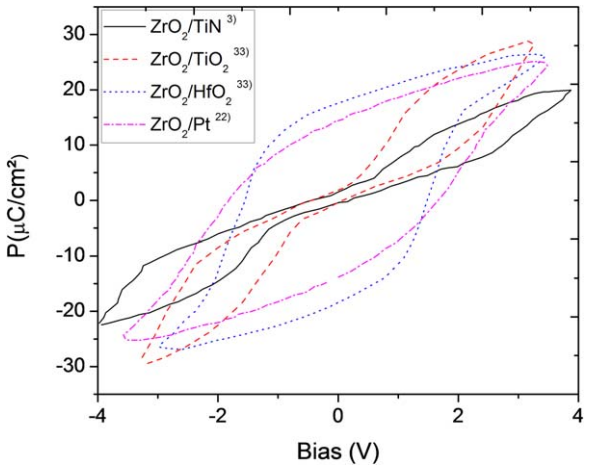

Fig. 4. (Color online) Polarization versus applied voltage hysteresis for ZrO_2 capacitors deposited by various authors[3,22,33] for different interface (with TiO_2 or HfO_2) and electrode conditions (TiN versus Pt).

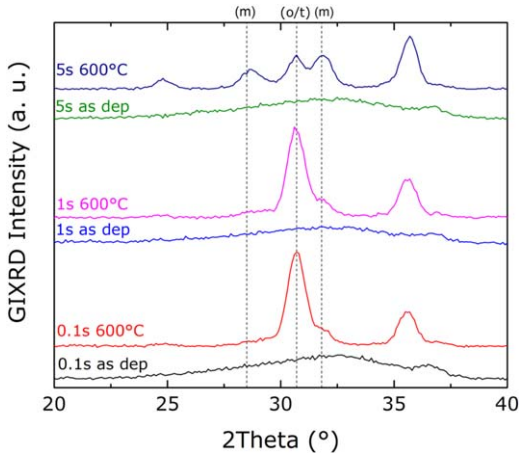

Fig. 5. (Color online) GIXRD diffraction pattern for pure HfO_2 deposited by ALD with different O_3 pulse times of 0.1–5 s. Patterns shown for as deposited layers and after 600 °C 20 s crystallization anneal in N_2.

Very short pulse times could lead to a higher carbon content in the layer due to an incomplete ligand removal. The carbon content was neglected in further discussion since similar studies for pure HfO_2 deposited by ALD in comparison to a carbon-free PVD process showed that a low carbon content did not influence the phase formation strongly.[16,17]

For pure HfO_2 the GIXRD patterns are displayed in Fig. 5 for different O_3 pulse times. A small shift of the 2-theta peak position at about 30.4°–30.8° related to the o/t-phase and an increase of the m-phase fraction (intensity at 28.5°, 31.6°) is visible for higher O_3 pulse times. Since a Rietveld refinement is difficult to perform for HZO films likely due to the later discussed different stress impact for different Hf/Zr content, the peak position and peak intensity is used to determine an estimate of the relative phase fraction. A Gaussian peak is fitted to the GIXRD intensity assuming a 2-theta peak of 30.4° for the o-phase and of 30.8° for the t-phase and an m-phase contribution at 28.5 and 31.6. Here, the distinction between the o- and t-phase is most critical. Since strain/stress can impact the GIXRD 2-theta peak position too, first a good correlation between the XRD peak position of the o-phase peak and remanent polarization values is verified. As visible in Fig. 6, results show the expected linear trend for the HZO layers and the resulting phase determination gives an estimate

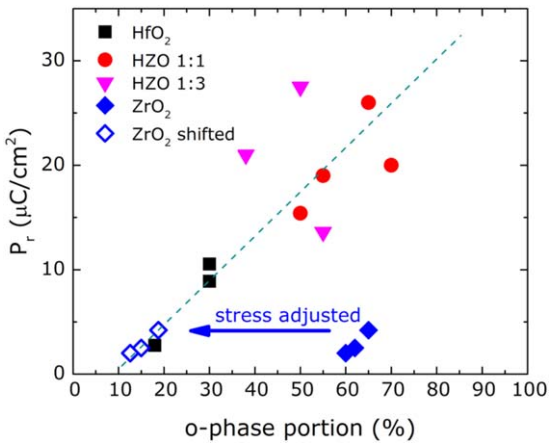

Fig. 6. (Color online) Remanent polarization P_r as a function of the o-phase fraction as determined by Gaussian fitting of the GIXRD patterns for different $Hf_xZr_{1-x}O_y$ compositions. Typically, a linear dependence is visible for all Hf/Zr compositions except pure ZrO_2. ZrO_2 values are adjusted assuming high hydrostatic tensile stress.

of the phase portions. A deviation in the linear trend appears only for the pure ZrO_2 films where lower P_r values are observed along with a decrease in the 2-theta position. Stress/strain is a possible reason for the shift in 2-theta position. Assuming that ZrO_2 should obey the same linear dependence of P_r on the o-phase fraction as the mixed $Hf_xZr_{1-x}O_2$ films, the observed P_r indicates the o-phase fraction would be at about 20% instead of 60% for the stressed pure ZrO_2.

Now GIXRD patterns for different Hf:Zr ratios (0%–75% ZrO_2 in HfO_2) and O_3 dose times are evaluated in Figs. 7(a)–7(c). For all different Hf:Zr ratios in mixed HZO films, a clear transition from a t-phase to a higher o-phase content and then subsequently to a higher m-phase fraction occurs for increasing O_3 dose times. Just the initial o/t/m-phase fraction is changing with higher ZrO_2 content from higher m-phase portions for pure HfO_2 to a high o-phase content for mixed HZO and then finally to an enhanced t-phase content for pure ZrO_2. Even though it is difficult to determine the real o/t ratio for pure ZrO_2 as expected from Fig. 6, results indicate that there is still a mixture of o- and t-phase present in pure ZrO_2 with about 20% o-phase content and not only non-polar phase t-portions as discussed in former reports.[2,4] Both the extracted and the possibly stress corrected value are shown in Fig. 7(d). As discussed above, the stress correction was performed by shifting the P_r values along the x-axis to match the linear P_r versus o-phase trend visible for all other Hf/Zr ratios in Fig. 6.

On the same structures polarization-voltage hysteresis loops are measured to verify the remanent polarization (P_r) value after 10^5 wake-up cycles with a bias field of +/− 3–4 MV cm^{-2} (Fig. 8). As indicated already from phase analysis, remanent polarization values start from different initial P_r values for low O_3 pulse times, go through a maximum of P_r before the value drops again for long O_3 pulses. Only for pure ZrO_2 just a slight increase of P_r for longer O_3 times is visible. Parallel to the phase change from the t- to o- to m-phase with increasing O content the according FE properties are determined.

The trend for ZrO_2 is consistent with PECVD results for ZrO_2 on Si substrates,[30] where a phase transition from t- to m-phase is reported, similar to values discussed for the pure

Final edited form was published in "Japanese Journal of Applied Physics". 2019, 58, S. SL0801-1 - SL0801-7. ISSN 1347-4065.
http://dx.doi.org/10.7567/1347-4065/ab45e3

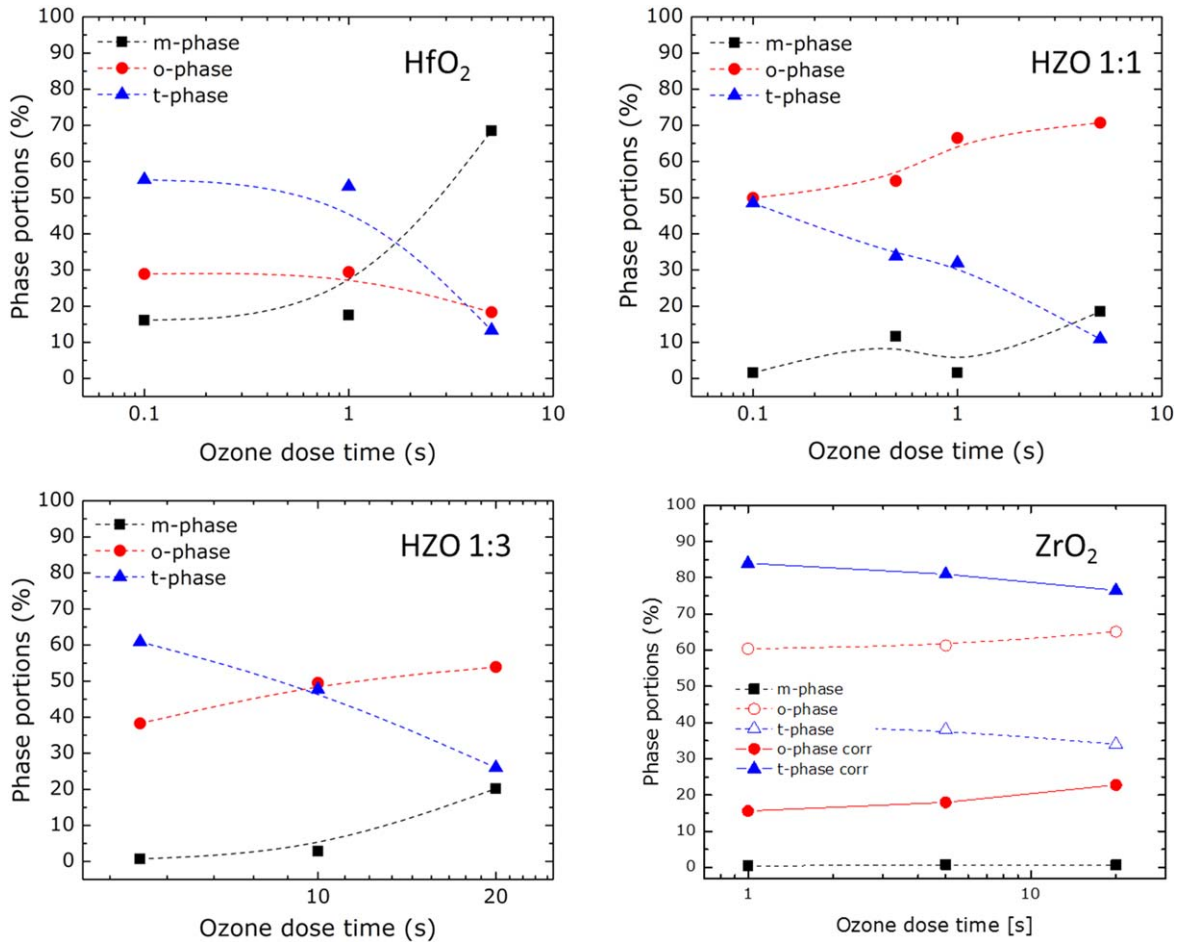

Fig. 7. (Color online) (a)–(d): Phase portions of the monoclinic, tetragonal, and orthorhombic phases in $Hf_xZr_{1-x}O_y$ as a function of the ozone dose time during ALD deposition: (a) pure HfO_2 (b) $Hf_{0.5}Zr_{0.5}O_2$ (c) $Hf_{0.25}Zr_{0.75}O_2$ (d) pure ZrO_2. Based on the discussion related to Fig. 6, stress corrected phase portions are presented in (d).

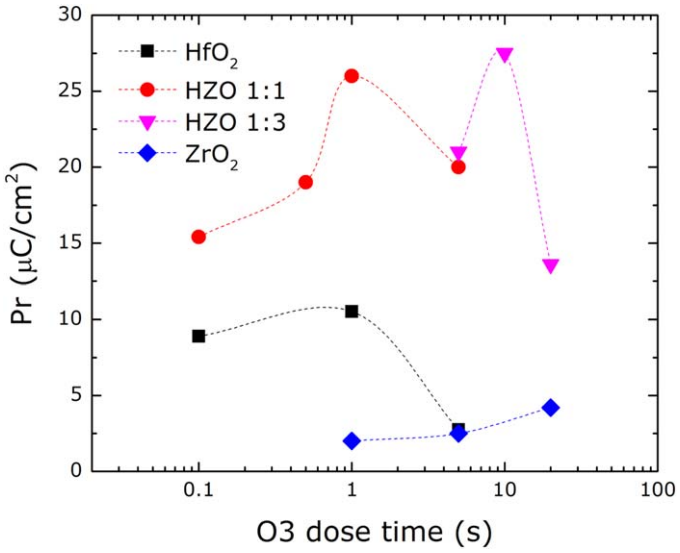

Fig. 8. (Color online) Remanent polarization P_r as a function of different O_3 dose times for pure HfO_2, $Hf_{0.5}Zr_{0.5}O_2$, $Hf_{0.25}Zr_{0.75}O_2$, and for pure ZrO_2.

HfO_2 system.[17] Furthermore, a polar o-phase was formed for ALD deposited ZrO_2 on Pt surfaces.[23] The use of TiN electrodes can cause scavenging of O from ZrO_2, which could keep the o-phase fraction low. In the Pt electrode case, less O scavenging is expected and a higher o-phase fraction could be formed[23] when the t-phase is less stabilized. In addition, Pt electrodes are enhancing the dissociation rate of O_3 or O_2 to atomic oxygen,[35] which enhances the reactivity of the oxygen precursor with the Zr precursor. As a result, also higher O amounts are expected in ZrO_2.

If results of Fig. 8 are plotted for different Hf/Zr content at constant O_3 dose time, different polarization versus ZrO_2 content relations would be achieved (e.g. see Fig. 10 for 5 s O_3 pulse time). As a result, the peak maximum of the P_r

Final edited form was published in "Japanese Journal of Applied Physics". 2019, 58, S. SL0801-1 - SL0801-7. ISSN 1347-4065.
http://dx.doi.org/10.7567/1347-4065/ab45e3

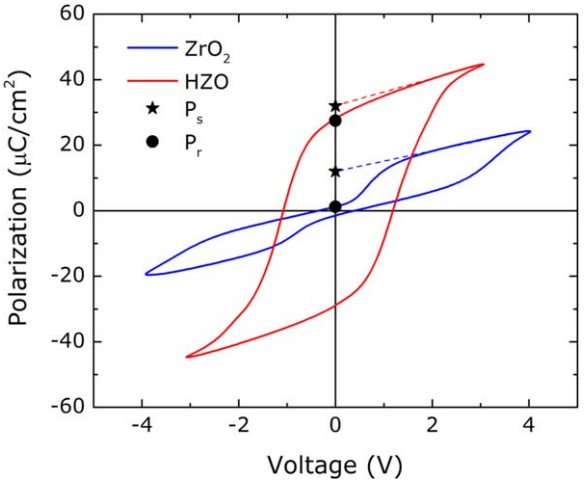

Fig. 9. (Color online) Polarization–voltage hysteresis for HZO and pure ZrO_2. Extracted values of the remanent and the spontaneous polarization values (P_r/P_s) are marked.

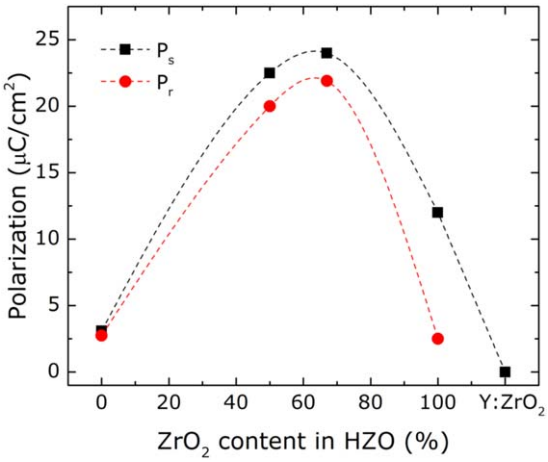

Fig. 10. (Color online) Remanent (P_r) and spontaneous polarization (P_s) as a function of different $Hf_xZr_{1-x}O_2$ composition.

versus ZrO_2 content is increasing for higher O_3 pulse times from 50% ZrO_2 content for 1 s O_3 to 75% ZrO_2 for 10 s O_3 pulse time. Values are added to results by other authors in Fig. 2. Accordingly, differences of various publications in Fig. 1 can be explained by different oxygen conditions in the ALD process. When extracting P_r values for different Hf/Zr content at an O_3 dose time of 5 s, the remanent polarization is going through a maximum value for an almost equal distribution of Hf and Zr (Fig. 10). For high Hf contents the polarization hysteresis loop is less pinched than for an enhanced Zr content (Figs. 9 and 10). Hence the P_r value drops to almost zero for pure ZrO_2, but the maximum polarization value (P_{max}) does not decrease in a similar way for pure ZrO_2 (Fig. 9). Subtracting the dielectric contribution from the pinched hysteresis loop, still a significant spontaneous polarization P_s of 12 $\mu C\,cm^{-2}$ is present which is roughly 50% of the value for HZO (Fig. 9). This reported trend is consistent with former publications (Fig. 1).[3,21] According to literature, an additional amount of t-phase stabilizing dopant (e.g. Y) in ZrO_2 is necessary to form the pure cubic/tetragonal phase.[14]

Hence, the origin of the pinched hysteresis loop needs to be discussed. In former reports, a field induced phase

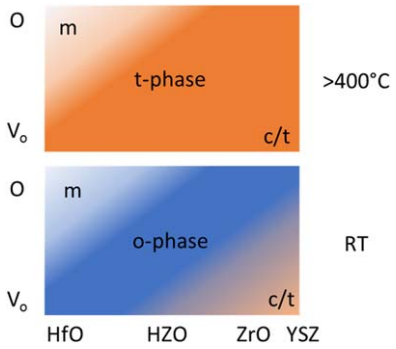

Fig. 11. (Color online) Schematic phase diagram with phase transformation during cool down from >400 °C (top) to room temperature (RT - bottom). Zr and O concentration (V_o=O deficient case) impact the phase transition. In a certain composition range the t-phase is transformed into the o-phase during cool down.

transition from the t- to o-phase was proposed.[3] But here in-operando XRD synchrotron measurements did not show any change of the XRD pattern,[36,37] when applying an external field to the structure. Hence, Hf positions with in the unit cell would be stable when an external field is applied and only a change in the O-positions can be proposed. Another reason for the pinched hysteresis shape could be a mixed o/t-phase as indicated from the 2-theta GIXRD analysis. Here, polar and non-polar regions would co-exist and the depolarization field could cause a reduction of P_r for low field conditions.[38] Non-polar regions could be present as interfacial layer to the electrodes[39] or with the bulk.[40] For zero external field, the depolarization field might be higher than the ferroelectric field and no ferroelectric polarization could be detected from the outside. By applying an external field, the depolarization field could be overcome and the polar properties become visible for higher fields. Due to the lower polar o-phase portion of ZrO_2 compared the HZO case, the P_s value would be reduced. This trend is visible in Fig. 9. Another possibility would be, that a different strained phase is formed for pure ZrO_2. A detailed structural characterization of the ZrO_2 layers is necessary to distinguish the last two cases.

Finally, a schematic phase diagram is presented for thin HZO films with different O content (Fig. 11). Hence, both O and Zr have an opposing impact on the phase formation where higher amounts of Zr and lower O concentrations can stabilize the t-phase in mixed HZO layers at film crystallization condition above 400 °C. Low oxygen contents have been shown to stem from higher oxygen vacancy concentrations.[17] Different authors determined the oxygen vacancy content as 0.3%–1%.[24,41] Depending on the layer composition, the t-phase transforms into the o-phase during cool down or the layer stays tetragonal. For low Zr and high O content, the m-phase is formed, which is stable during cooling.[42,43] Overall, higher O-amounts would rather stabilize the m-phase in contrast to higher Zr amounts resulting in higher t-phase portions. Looking at the crystallization in as deposited films, O enhancement reduces the crystallization temperature and with this an increase in the m-phase portion is present. This effect is enhanced for higher ZrO_2 content in HZO.[44] Overall, the increased O_3 pulse time had a stronger impact in mixed HZO films in contrast to pure HfO_2 or ZrO_2 layers (Fig. 8). Here, the impact is stronger for HfO_2

Final edited form was published in "Japanese Journal of Applied Physics". 2019, 58, S. SL0801-1 - SL0801-7. ISSN 1347-4065.
http://dx.doi.org/10.7567/1347-4065/ab45e3

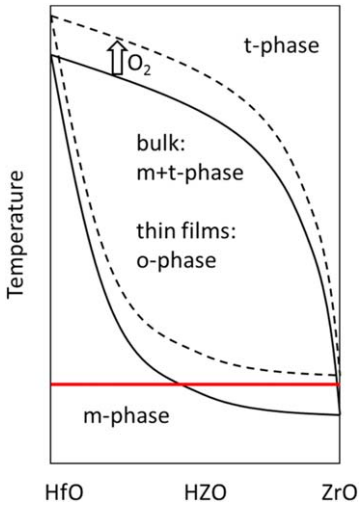

Fig. 12. (Color online) Schematic phase diagram as reported for bulk HZO[19] in combination with expected phase diagram for thin HZO layers. Impact of additional oxygen during deposition added to the diagram. Red line indicates the room temperature condition for thin films or 1100 °C for bulk material.[19]

compared to ZrO_2. These results fit nicely to reported HZO phase diagrams[19] (Fig. 12). For the bulk case, HfO_2 crystallize predominately in the m and ZrO_2 in the t-phase. A mixed m+t-phase is described for the HZO system. A similar schematic phase diagram is expected with the o-phase for thin HZO layers. Oxygen addition would shift the phase diagram to higher temperatures. At room temperature (red line in Fig. 12), a phase change from a t-phase to m-phase with additional oxygen can be observed.

4. Conclusions

$Hf_xZr_{1-x}O_y$ thin films have been reviewed with a focus on the composition and influence of oxygen on the formation of crystal phases and ferroelectric properties. To clarify the ambiguity of the distinct influences of Zr and oxygen reported by different authors, experiments were undertaken, which showed that the effect of oxygen can influence the phase formation process for the Hf-Zr stoichiometry range in $Hf_xZr_{1-x}O_2$. Thus, during deposition of a HZO layer both the oxygen and Zr content can be varied in the FE layer within a capacitor structure. An optimized polar orthorhombic phase fraction can be reached for a certain Zr and O level in the layer. In pure HfO_2 thin films, predominately m-phase portions are present that change to the polar o-phase for higher Zr content and finally to a mixed o/t-phase for pure ZrO_2. Only further doping by a c/t-phase stabilizing dopant like Y can form a completely non-polar ZrO_2 phase. The oxygen level within the layer can directly influence the Hf/Zr ratio with maximum polarization condition. Accordingly, Zr and O have an opposing impact on the phase formation. In contrast, both Zr and O addition lowers the crystallization temperature of HfO_2. Structural results of processed ALD films correlate nicely to former publications for PVD, PLD, and PECVD deposited $Hf_xZr_{1-x}O_2$ layers.

Acknowledgments

P.D.L is funded by the German Ministry of Economic Affairs and Energy (BMWi) project (16IPCEI310). A.T. is grateful for the TU-Dresden Fellowship.

ORCID iDs

Uwe Schroeder https://orcid.org/0000-0002-6824-2386

1) T. S. Böscke, J. Müller, D. Bräuhaus, U. Schröder, and U. Böttger, Appl. Phys. Lett. **99**, 102903 (2011).
2) T. Mikolajick, S. Slesazeck, M. H. Park, and U. Schroeder, MRS Bull. **43**, 340 (2018).
3) J. Mueller, T. S. Boescke, U. Schroeder, S. Mueller, D. Braeuhaus, U. Boettger, L. Frey, and T. Mikolajick, Nano Lett. **12**, 4318 (2012).
4) S. Mueller, C. Adelmann, A. Singh, S. Van Elshocht, U. Schroeder, and T. Mikolajick, ECS J. Solid State Sci. Technol. **1**, N123 (2012).
5) U. Schroeder et al., Inorg. Chem. **57**, 2752 (2018).
6) S. Mueller, J. Mueller, A. Singh, S. Riedel, J. Sundqvist, U. Schroeder, and T. Mikolajick, Adv. Funct. Mater. **22**, 2412 (2012).
7) M. H. Park, T. Schenk, and U. Schroeder, *Ferroelectricity in Doped Hafnium Oxide: Materials, Properties, and Devices* (Elsevier, Amsterdam, 2019), Chap. 3.1, p. 49.
8) A. Toriumi, L. Xu, S. Shibayama, and S. Migita, *Ferroelectricity in Doped Hafnium Oxide: Materials, Properties, and Devices* (Elsevier, Amsterdam), Chap. 3.3, p. 103.
9) T. Shimizu and H. Funakubo, *Ferroelectricity in Doped Hafnium Oxide: Materials, Properties, and Devices* (Elsevier, Amsterdam, 2019), Chap. 4, p. 173.
10) U. Boettger, S. Starschich, D. Griesche, and T. Schneller, *Ferroelectricity in Doped Hafnium Oxide: Materials, Properties, and Devices* (Elsevier, Amsterdam, 2019), Chap. 3.4, p. 127.
11) T. Mimura, K. Katayama, T. Shimizu, H. Uchida, T. Kiguchi, A. Akama, T. J. Konno, O. Sakata, and H. Funakubo, Appl. Phys. Lett. **109**, 052903 (2016).
12) S. J. Kim et al., Appl. Phys. Lett. **111**, 242901 (2017).
13) M. H. Park, T. Schenk, C. S. Hwang, and U. Schroeder, *Ferroelectricity in Doped Hafnium Oxide: Materials, Properties, and Devices* (Elsevier, Amsterdam, 2019), Chap. 8, p. 341.
14) S. Shibayama, T. Nishimura, S. Migita, and A. Toriumi, J. Appl. Phys. **124**, 184101 (2018).
15) M. H. Park, T. Schenk, S. Starschich, C. M. Fancher, H. J. Kim, U. Boettger, C. S. Hwang, A. Toriumi, X. Tian, and U. Schroeder, *Ferroelectricity in Doped Hafnium Oxide: Materials, Properties, and Devices* (Elsevier, Amsterdam, 2019), Chap. 3.5, p. 145.
16) A. Pal, V. K. Narasimhan, S. Weeks, K. Littau, D. Pramanik, and T. Chiang, Appl. Phys. Lett. **110**, 022903 (2017).
17) T. Mittmann et al., Adv. Mater. Interfaces **6**, 1900042 (2019).
18) L. Wang, H. P. Li, and R. Stevens, J. Mater. Sci. **27**, 5397 (1992).
19) E. I. Zoz and A. G. Karaulov, *ACerS—NIST, Phase. Equilibria. Diagrams* (The American Ceramic Society, Westerville, OH, 2014), Refract., 32, 109 (1991).
20) M. Yashima, S. Sasaki, M. Kakihana, Y. Yamaguchi, and M. Yoshimura, Acta Crystallogr. **BS0**, 663 (1994).
21) M. H. Park, H. J. Kim, K. D. Kim, Y. H. Lee, S. D. Hyun, and C. S. Hwang, *Ferroelectricity in Doped Hafnium Oxide: Materials, Properties, and Devices* (Elsevier, Amsterdam, 2019), Chap. 3.2, p. 75.
22) Y. W. Lu, J. Shieh, and F. Y. Tsai, Acta Mater. **115**, 68e75 (2016).
23) T. Y. Hsu, B. T. Lin, J. Shieh, and M. J. Chen, Proc ASME, San Antonio, 2018.
24) W. Hamouda, A. Pancotti, C. Lubin, L. Tortech, C. Richter, U. Schroeder, and N. Barrett, submitted to J. Appl. Phys.
25) D. Y. Cho et al., Chem. Mater. **24**, 3534 (2012).
26) S. Y. Lee, H. K. Kim, J. H. Lee, I. H. Yu, J. H. Lee, and C. S. Hwang, J. Mater. Chem. C **2**, 2558 (2014).
27) S. U. Sharath, J. Kurian, P. Komissinskiy, E. Hildebrandt, T. Bertaud, C. Walczyk, P. Calka, T. Schroeder, and L. Alff, Appl. Phys. Lett. **105**, 073505 (2014).
28) S. U. Sharath et al., Appl. Phys. Lett. **104**, 063502 (2014).
29) K. Takada, Y. Saho, T. Yoshimura, and N. Fujimura, Jpn. J. Appl. Phys. **58**, SLLB03 (2019).
30) B. O. Cho, J. P. Chang, J. H. Min, S. H. Moon, Y. W. Kim, and I. Levin, J. Appl. Phys. **93**, 745 (2003).
31) T. Mittmann, F. P. G. Fengler, C. Richter, M. H. Park, T. Mikolajick, and U. Schroeder, Microelectron. Eng. **178**, 48 (2017).
32) S. W. Smith, A. R. Kitahara, M. A. Rodriguez, M. D. Henry, M. T. Brumbach, and J. F. Ihlefeld, Appl. Phys. Lett. **110**, 072901 (2017).
33) S. H. Yi, B. T. Lin, T. Y. Hsu, J. Shieh, and M. J. Chen, J. Eur. Ceram. Soc. **39**, 4038 (2019).

Final edited form was published in "Japanese Journal of Applied Physics". 2019, 58, S. SL0801-1 - SL0801-7. ISSN 1347-4065.
http://dx.doi.org/10.7567/1347-4065/ab45e3

34) M. A. Rahman, S. Rout, J. P. Thomas, D. McGillivray, and K. T. Leung, J. Am. Chem. Soc. **138**, 11896 (2016).
35) S. L. Bernasek and G. A. Somorjai, Surf. Sci. **48**, 204 (1975).
36) M. Hoffmann et al., J. Appl. Phys. **118**, 072006 (2015).
37) T. Schenk, S. Grofman, T. Mikolajick, and U. Schroeder, submitted to Adv. Material Interfaces.
38) P. D. Lomenzo, C. Richter, S. Slesazeck, T. Mikolajick, and U. Schroeder, submitted to ACS Nano.
39) E. D. Grimley, T. Schenk, X. Sang, M. Pešić, U. Schroeder, T. Mikolajick, and J. M. LeBeau, Adv. Electron. Mater. **2**, 1600173 (2016).
40) F. Mehmood, M. Hoffmann, P. D. Lomenzo, C. Richter, M. Materano, T. Mikolajick, and U. Schroeder, Adv. Mater. Interfaces 1901180 (2019).
41) F. P. G. Fengler, R. Nigon, P. Muralt, E. D. Grimley, X. Sang, V. Sessi, R. Hentschel, J. M. LeBeau, T. Mikolajick, and U. Schroeder, Adv. Electron. Mater. **4**, 1700547 (2018).
42) M. H. Park, Y. H. Lee, H. J. Kim, Y. J. Kim, T. Moon, K. D. Kim, S. D. Hyun, T. Mikolajick, U. Schroeder, and C. S. Hwang, Nanoscale **10**, 716 (2018).
43) M. H. Park, Y. H. Lee, T. Mikolajick, U. Schroeder, and C. S. Hwang, Adv. Electron. Mater. **5**, 1800522 (2019).
44) M. Materano, C. Richter, T. Mikolajick, and U. Schroeder, in preparation.